

Classical Contrast Enhancement Methods in the Classification of Estrous Cycle Images

Rocio Ochoa-Montiel^{1,2}, Ismael Llamur³,
Humberto Sossa^{1,4}, Gustavo Olague⁵

¹ Instituto Politécnico Nacional,
Centro de Investigación en Computación,
Mexico

² Universidad Autónoma de Tlaxcala,
Facultad de Ciencias Básicas,
Mexico

³ Universidad Nacional de Tucuman,
Facultad de Ciencias Exactas y Tecnologías,
Argentina

⁴ Tecnológico de Monterrey,
Escuela de Ingeniería y Ciencias,
Mexico

⁵ Centro de Investigación Científica y de Educación Superior de Ensenada,
EvoVision Laboratory Ensenada,
Mexico

{ma.rocio.ochoa, ismaelllamur013, humbertosossa,
gustavo.olague}@gmail.com

Abstract. In the biological area, the short reproductive cycle in rodents is useful because it allows analyzing electrophysiological properties, behaviors, or drugs effects, through the changes observed during this period. This cycle is composed of 4 stages, in which the classification is determined by vaginal cytology. Although automatic approaches have been used for the recognition of these stages, they are computationally expensive and require a great number of images for adequate performance. In this work, we study the effect of contrast enhancement on the images classification of the reproductive cycle named estrous cycle. We use a dataset of 344 images and four classical contrast enhancement methods. We extract texture features and use four classifiers to evaluate the impact of the contrast enhancement methods. From the results, we find that the contrast enhancement methods that do not emphasize strongly some regions in the images show higher classification results than those yes do it. Furthermore, features extracted manually overcome the classification rate concerning the features extracted automatically with a standard convolutional neural network.

Keywords: Contrast enhancement, classification, estrous cycle.

1 Introduction

Artificial vision has a wide variety of applications in diverse fields like surveillance, security or medicine [5, 7]. In Biology, the analysis of rodent tissues is especially useful to study physiological processes due to these are carrying on short periods. Particularly, reproduction is an ideal process for researching changes along a cycle, such as fertility rates, effects of treatments, or environmental diverse conditions, among others [13, 10]. The reproductive cycle in rodents named the estrous cycle is formed by four phases: proestrus P, estrus E, metestrus M, and diestrus D.

Knowledge of these stages is important for interpretations of female animals' data, whereas their identification is through the observation of cells in vaginal smears where properties like type, number, shape, size, and proportion of cells are evaluated [2, 4]. Nevertheless, the recognition of estrous cycle stages by a human expert takes a long time, and the evaluations are frequently subjective due to differences of skill of the examiners. We assume this is one of the main reasons why the automatic recognition problem has been poorly addressed, since the amount of correctly labeled data is critical for the good performance of these approaches.

In this regard, [9] presents a quantitative method for assessing Estrous cycle stages. However, the method focuses on showing trends between diverse cell types in each stage. On the other hand, authors in [12] propose software that enables more efficient cycle stage data analysis and pattern visualization, while in [8] the visual classification of the estrous cycle images is addressed by using support vector machines, multilayer perceptron networks, and convolutional neural networks.

On the other hand, [14] proposes the deep learning-based classification of the estrous cycle, considering only three stages of the cycle. In this work, for the first time we evaluate some classical contrast enhancement methods on the classification of estrous cycle images. It is important to mention that our objective is to know the impact of these methods, and not to exceed the classification rate of previous works [8, 14]. In the next section, the materials and methods are described. Section 3 presents the proposed methodology. In section 4, experiments and results are shown. Conclusions are included in section 5.

2 Materials and Methods

2.1 Contrast Enhancement Methods

The simplest kinds of image processing are point methods, where each output pixel value depends on an input pixel value; including some globally recovered information or parameters. Common techniques of image enhancement as histogram equalization (HE), adaptive histogram equalization (AHE), and local saturation (LS) are in this category.

We decided to use these because the aim is to enhance details over small or regular areas in the images [15]. HE enhances the contrast of images by transforming the values in an intensity image so that the histogram of the output image approximately matches a specified histogram, uniform distribution by default. Whereas, AHE performs contrast-limited adaptive histogram equalization.

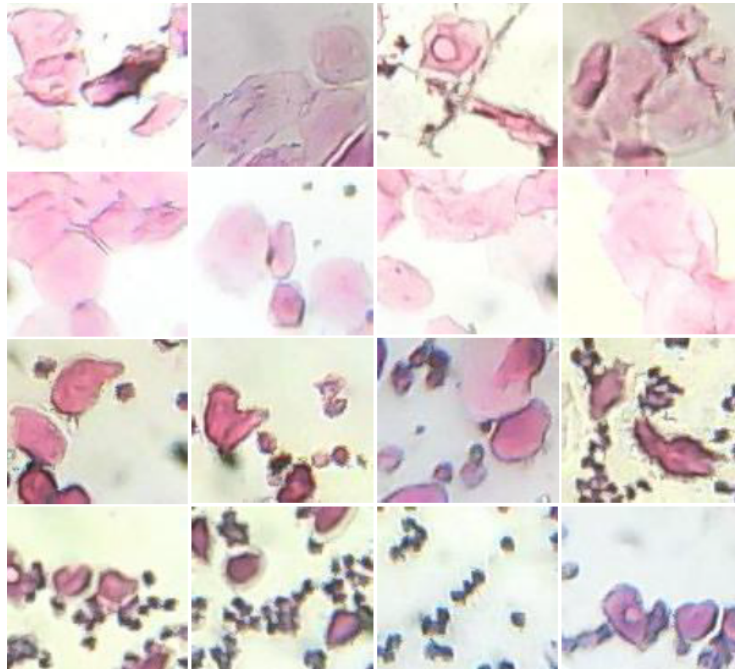


Fig. 1. Representative cells of the stages of reproductive cycle in rats. Images in each row depict the each cycle stage: row 1-stage P, row 2-stage E, row 3-stage M and row 4-stage D.

Unlike HE, it operates on small data regions (tiles) rather than the entire image. Each tile's contrast is enhanced so that the histogram of each output region approximately matches the specified histogram, typically a uniform distribution. The contrast enhancement can be limited to avoid amplifying the noise which might be present in the image. On the other hand, LS increases the image contrast by mapping the values of the input intensity image to new values, hence $n\%$ of the data is saturated at low and high intensities of the input data.

Furthermore, we use an automatic contrast enhancement (ACE) proposed in previous work [11], which enhances the contrast on local areas through a histogram approximation using differential evolution. An advantage of this method is the possibility of defining in which areas of the image we want to contrast enhancement. Thus, clearer or darker regions (Cr or Dr) can be selected for the enhancement.

2.2 Classifiers

The most of classifiers used in machine learning require features extracted previously in a manual or semi-automatic way. Classifiers as multilayer perceptron (MLP), random forest (RF), and the smooth dendrite morphological neurons (SDMN) are of this type. The firsts are known for their good performance in diverse applications, whereas the SDMN is a last generation net recently proposed by [6] that has a good generalization capacity.

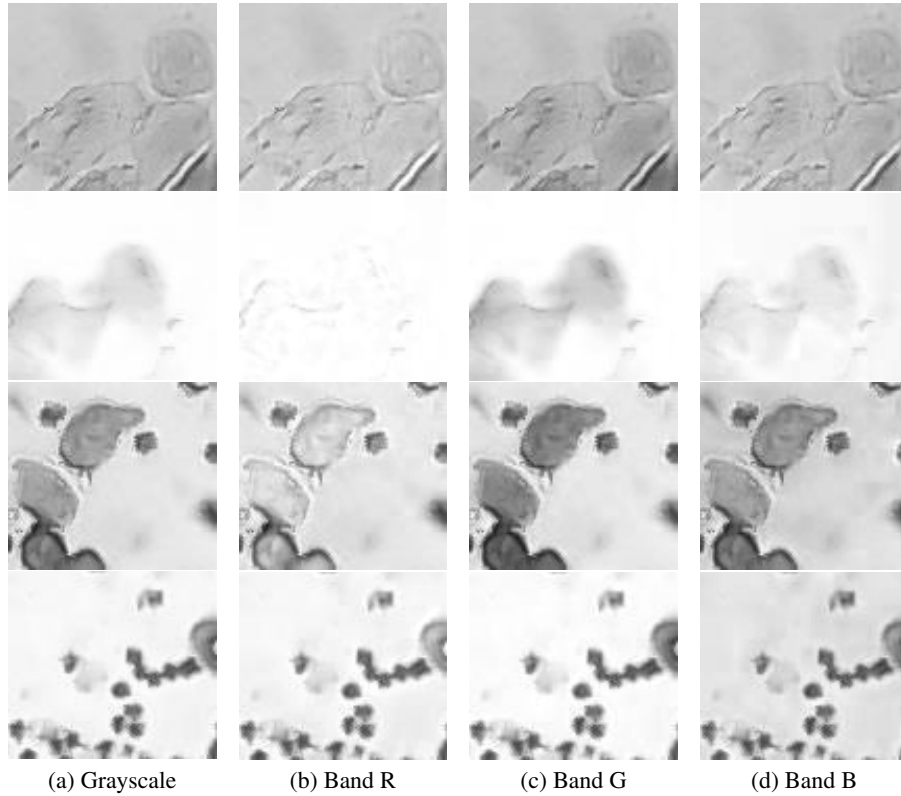


Fig. 2. Images of bands R, G, B. Each row depict a cycle stage: row 1-stage P, row 2-stage E, row 3-stage M and row 4-stage D.

On the other hand, the convolutional neural networks (CNNs) are the approaches most representative of automatic classification due to they automatically extract features and perform classification. These models do not need previous image processing or explicit feature extraction. Instead, they use the image to find adequate descriptors for image classification. Thus, it is assumed that the learning occurs by using the position of patterns directly from the input image data exclusively, without considering previous knowledge about this.

3 The Proposed Methodology

In this work we use a balanced dataset of 344 images with 86 for each stage of the estrous cycle. Images were acquired with an optical microscope using a magnification of 400X and a camera Logitech C170. These images are in .jpg format with a resolution of 100×90 . Fig. 1 presents images RGB for each stage. From the dataset, we use the G band images because this shows better contrast concerning the R and B bands, as is shown in Fig. 2.

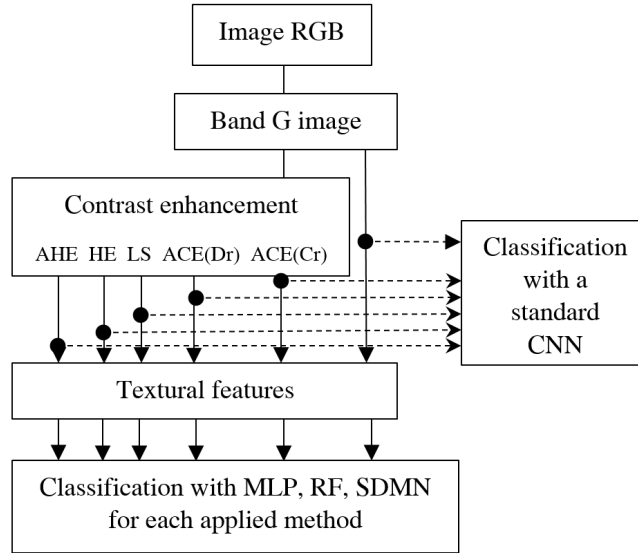


Fig. 3. General flowchart of the proposed methodology.

First, we apply the contrast enhancement methods mentioned in the previous section. In addition, we consider images without applying the contrast enhancement to compare. After that, textural features based on the gray level co-occurrence matrix (GLCM) are extracted. These features are used by the classifiers MLP, RF, and SDM to know the advantages of the contrast enhancement methods in image classification. On the other hand, to compare with an automatic classification method, we use a standard CNN. We assess the classification performance for each image class P, E, M, and D, which depict the four phases of the estrous cycle. In this way, to test the classifiers MLP, RF, and SDM we use textural features since the images are in grayscale; whereas CNN uses the images directly. Fig. 3 shows the general flowchart of the proposed methodology.

4 Experiments and Results

The experiments were performed on a CPU Intel Core i9- 7900X, 64GB RAM, Windows10 Enterprise Edition operating system, graphics processing unit (GPU) GeForceGTX 1080, and MATLAB.

4.1 Datasets

Datasets used in the experiments are built applying the contrast enhancement methods ACE (Cr , and Dr), HE, AHE, and LS from section 2. ACE was implemented according to [11], and the methods remainder are computed with the functions *histeq*, *adapthisteq*, and *imadjust*, respectively from the image processing toolbox of Matlab.

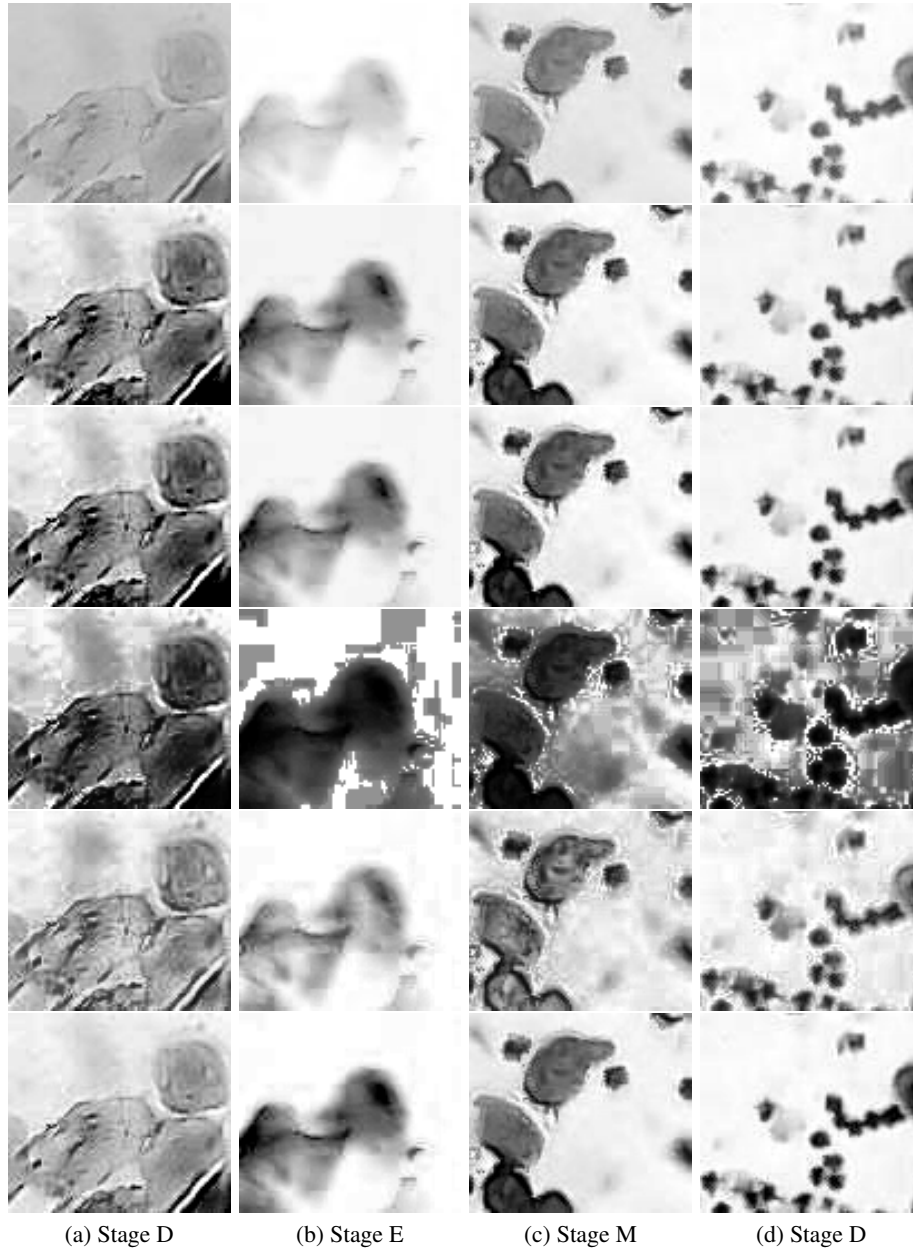


Fig. 4. Images of datasets used. Row 1. Band G, row 2. ACE (Cr), row 3. ACE (Dr), row 4. HE, row 5. AHE, and row 6. LS.

Additionally, a dataset is built from the images of band G without applying contrast enhancement. In this way, we obtain six datasets for the experiments. Fig. 4 shows the images obtained from the methods applied.

Table 1. Results of classification.

Method	SDMN		MLP		RF		CNN	
	Accuracy (%)	s.d	Accuracy (%)	s.d	Accuracy (%)	s.d	Accuracy (%)	s.d
Band G	62.50	±3.55	69.23	±4.04	64.42	±2.82	68.27	±4.26
AHE	68.33	±4.88	70.19	±3.91	61.54	±1.78	62.50	±7.74
HE	61.67	±3.01	53.85	±3.04	55.77	±2.43	49.04	±9.27
LS	69.17	±5.18	67.31	±2.80	69.23	±3.43	58.65	±5.04
ACE (Dr)	69.17	±4.90	63.46	±1.50	61.54	±2.87	48.08	±5.64
ACE (Cr)	71.25	±4.49	67.31	±3.71	61.54	±2.02	48.08	±8.19
Average	67.02	±4.34	65.23	±3.17	62.34	±2.56	55.77	±6.69
Min	61.67	±3.01	53.85	±1.5	55.77	±1.78	48.08	±4.26
Max	71.25	±5.18	70.19	±4.04	69.23	±3.43	68.27	±9.27

4.2 Feature Extraction and Classification

The textural features for the tests with MLP, RF, and SDMN are computed from the gray level-co-occurrence using eight gray levels. Because the GLCM probabilities represent the conditional joint probabilities of all pairwise combinations of gray levels in the spatial windows of interest given the parameters interpixel distance (δ) an orientation (θ), we adjust $\delta = 1$, and $\theta = \{0, 45, 90, 135, 180\}$. We use seven shift-invariant features suggested by [3]: uniformity, entropy, dissimilarity, inverse difference, inverse difference moment, and correlation. These features are computed for each value of θ .

Later, we average the four interpixel orientations for each feature, thus we obtain seven features for each image. These features are used independently by each classifier. For the MLP, we consider one hidden layer with 50 neurons and the activation function `traingdx` from the Matlab toolbox. RF was initialized with 500 trees and the classification is performed by majority vote as in [1]. Finally, SDMN was used with the parameters suggested in [6]. For the experiments with the CNN, we use a structure composed by four convolutional and max-pooling layers.

The feature maps are flattened and reduced to an output of size four. Data augmentation is used on the training set. The augmentation operations include horizontal and vertical reflexion. Accordingly, we have the addition of a random number of augmented images to the training set in each epoch. The number of filters in the four convolutional layers are 4, 8, 16, and 32. The training process is stopped when the validation loss does not decrease for 20 epochs. In all experiments, we use 50% of data for training, 20% for validation, and the remainder for testing.

Five-fold cross-validation is used to assess the training performance, and the best net model from the five-fold validation is selected and used with the test set to assess the net performance. To evaluate the global classification performance, we repeat the experiment ten times. Results of classification experiments for the datasets—Band G, AHE, HE, LS, ACE(Dr), ACE(Cr)— are presented in Table 1. Note that results in ACE(Cr) reached the best performance.

				%Acc./class
45	1	8	6	94.11
0	55	0	5	66.66
12	1	38	9	72.22
8	10	9	33	76.47

Fig. 5. Confusion matrix of the best solution. Row1: stage P, Row2: stage E, Row3: stage M, Row4: stage D.

In general the methods in which the output image does not tend to binarization are adequate for classifying when texturales features are used. On the other hand, the average by classifier shows that classifiers with better performance are SDMN and MLP, whereas the worst performance is achieved by the CNN.

Furthermore, we show in Fig. 5 the confusion matrix for the best solution (this is, accuracy=71.25 for SDMN in Table 1). We observed that the stage P is the best recognized, while the stage E obtains poor classification results. Regard CNN, the features are automatically extracted by the net, and the contrast enhancement methods are not useful for classifying, as we can see Table 1. Finally, it is to note that method HE shows poor performance in all tests.

5 Conclusions

This work proposes for the first time the use of contrast enhancement methods for classifying the four stages in the reproductive cycle on rodents. The methodology proposed is inspired by previous works, in which the main objective is to improve the classification rate. Although this aim is important, in this work we focus on knowing the impact of classical contrast enhancement methods for the estrous cycle image classification.

From the results, we suggest that using contrast enhancement methods is useful when features are extracted manually to be used by classifiers. While for the automatic classifiers these methods are not useful. In a future work, we like to improve the classification rate, and to evaluate another automatic classification methods.

Acknowledgments. Authors would like to acknowledge the support provided by the Instituto Politécnico Nacional under projects: SIP 20200630 and SIP 20210788, CONACYT under projects: 65 (Fronteras de la Ciencia) and 6005 (FORDECYT-PRONACES), and CICESE through the project 634-135 to carry out this research. First author thanks the Autonomous University of Tlaxcala, Mexico for the support. Authors also express their gratitude to the Applied Computational Intelligence Network (RedICA).

References

1. Breiman, L.: Random forests. *Machine Learning*, vol. 45, no. 1, pp. 5–32 (2001) doi: 10.1023/A:1010933404324

2. Byers, S., Wiles, M., Sadie, D., Taft, R.: Mouse estrous cycle identification tool and images. *PloS one*, vol. 7, pp. e35538 (2012) doi: 10.1371/journal.pone.0035538
3. Clausi, D.: An analysis of co-occurrence texture statistics as a function of grey level quantization. *Canadian Journal of Remote Sensing*, vol. 28 (2002) doi: 10.5589/m02-004
4. Cora, M., Kooistra, L., Travlos, G.: Vaginal cytology of the laboratory rat and mouse: Review and criteria for the staging of the estrous cycle using stained vaginal smears. *Toxicologic pathology*, vol. 43 (2015) doi: 10.1177/0192623315570339
5. Doan, M., Case, M., Masic, D., Hennig, H., McQuin, C., Caicedo, J., Singh, S., Goodman, A., Wolkenhauer, O., Summers, H., et al.: Label-free leukemia monitoring by computer vision. *Cytometry. Part A : the journal of the International Society for Analytical Cytology*, vol. 97, no. 4, pp. 407–414 (2020) doi: 10.1002/cyto.a.23987
6. Gómez-Flores, W., Sossa, H.: Smooth dendrite morphological neurons. *Neural Networks*, vol. 136, pp. 40–53 (2021) doi: 10.1016/j.neunet.2020.12.021
7. Hemaanand, M., Kumar, V., Karthika, R.: Smart surveillance system using computer vision and internet of things. *Journal of Computational and Theoretical Nanoscience*, vol. 17, pp. 68–73 (2020) doi: 10.1166/jctn.2020.8631
8. Hernández Hernández, G., Delgado Toral, L., Ochoa Montiel, M. R., Zamora Gómez, E., Sossa, H., Barreto Flores, A., Ramos Collazo, F., Reyes Luna, R.: Estrous cycle classification through automatic feature extraction. *Computacion y Sistemas*, vol. 23, no. 4, pp. 1249–1259 (2019) doi: 10.13053/cys-23-4-3095
9. Hubscher, C., Brooks, D., Johnson, J.: A quantitative method for assessing stages of rat estrous cycle. *Biotechnic & histochemistry : official publication of the Biological Stain Commission*, vol. 80, pp. 79–87 (2005) doi: 10.1080/10520290500138422
10. Kaur, S., Benton, W. L., Tongkhuya, S. A., Lopez, C. M., Uphouse, L., Averitt, D. L.: Sex differences and estrous cycle effects of peripheral serotonin-evoked rodent pain behaviors. *Neuroscience*, vol. 384, pp. 87–100 (2018) doi: 10.1016/j.neuroscience.2018.05.017
11. Ochoa-Montiel, R., Olague, G., Sossa, H.: Expert knowledge for the recognition of leukemic cells. *Applied Optics*, vol. 59, no. 14, pp. 4448–4460 (2020) doi: 10.1364/AO.385208
12. Pantier, L., Li, J., Christian, C.: Estrous cycle monitoring in mice with rapid data visualization and analysis. *Bio-Protocol*, vol. 9, no. 17, pp. e3354 (2019) doi: 10.21769/BioProtoc.3354
13. Priddy, B., Carmack, S., Thomas, L., Vendruscolo, J., Koob, G., Vendruscolo, L.: Sex, strain, and estrous cycle influences on alcohol drinking in rats. *Pharmacology Biochemistry and Behavior*, vol. 152 (2016) doi: 10.1016/j.pbb.2016.08.001
14. Sano, K., Matsuda, S., Tohyama, S., Komura, D., Shimizu, E., Sutoh, C.: Deep learning-based classification of the mouse estrous cycle stages. *Scientific Reports*, vol. 10, no. 1, pp. 11714 (2020) doi: 10.1038/s41598-020-68611-0
15. Szeliski, R.: *Computer Vision. Algorithms and Applications* (2011)